

Supporting Information for

The Biginelli Reaction under Batch and Continuous Flow Conditions:
Catalysis, Mechanism and Antitumoral Activity

Gabriel C. O. Silva,^a Jose R. Correa,^b Marcelo O. Rodrigues,^{a} Haline G. O. Alvim^b Bruna C. Guido,^b
Claudia C. Gatto,^{a,b} Kaline A. Wanderley,^a Mariana Fioramonte,^c Fabio C. Gozzo,^c Rodrigo O. M. A. de
Souza,^d and Brenno A. D. Neto,^{b*}*

^a LIMA-Laboratório de Inorgânica e Materiais, Campus Universitário Darcy Ribeiro, CEP 70904970, P.O.Box 4478, Brasília-DF, Brazil.

^b Laboratory of Medicinal and Technological Chemistry, University of Brasilia (IQ-UnB). Campus Universitario Darcy Ribeiro, CEP 70904970, P.O.Box 4478, Brasília-DF, Brazil.

^c Institute of Chemistry, University of Campinas (Unicamp), Campinas, São Paulo 13083-970, Brazil.

^d Biocatalysis and Organic Synthesis Group, Chemistry Institute, Federal University of Rio de Janeiro, Brazil.

KEYWORDS. Metal-organic frameworks, Heterogeneous catalysis, X-ray, Multicomponent reaction, Biginelli reaction, Mechanism, Mass spectrometry.

Experimental Section

A suitable crystal of each MOF (**1** and **2**) was selected under a polarizing microscope and glued in a thin glass fiber. The crystallographic data were collected in a Bruker SMART CCD APEX II area detector diffractometer with graphite-monochromated Mo *K* α radiation ($\lambda = 0.71073 \text{ \AA}$) at room temperature ($T = 293 \text{ K}$), operating at 20 kV and 5 mA. The structures were determined and refined using SHELEX-HHHH. All hydrogen atoms were located in difference Fourier maps. In the final refinement all hydrogen atoms were geometrically placed and held in a rigid mode. Additionally, the refinements have included isotropic thermal parameter for hydrogen atoms and anisotropic thermal parameter for all the non-hydrogen atoms.

ESI-MS and ESI-MS/MS measurements were performed in the positive ion mode (m/z 50-2000 range) on a Synapt HDMS instrument (Waters Co.). This instrument has a hybrid quadrupole/ion mobility/orthogonal acceleration time-of-flight (oa-TOF) geometry and was used in the TOF V+ mode. All samples were dissolved in methanol to form 50 μM solutions and were directly infused into the ESI source at a flow rate of 10 $\mu\text{L}/\text{min}$ after 5 minutes at 90 $^{\circ}\text{C}$. ESI source conditions were as follows: capillary voltage 3.0 kV, sample cone 20 V, extraction cone 3 V.

NMR spectra were recorded on a 7.05 T instrument using a 5-mm internal diameter probe operating at 300 MHz for ^1H and at 75 MHz for ^{13}C . Chemical shifts were expressed in parts per million (ppm) and referenced by the signals of the residual hydrogen atoms of the deuterated solvent (DMSO- d_6), as indicated in the legends.

Photoluminescence spectra were collected using a FLUOROLOG3 ISA/Jobin-Yvon spectrofluorometer equipped with Hamamatsu R928P photomultiplier a SPEX 1934 D phosphorimeter, a 450 W Xe arc lamp and a pulsed 150W Xe-Hg lamp. All spectra were corrected for the spectral response of the monochromators and the detector corrected via correction spectra provided by the manufacturer. Thermogravimetric and Differential Thermal Analysis (TGA/DTA) curves were performed using a Shimadzu Simultaneous TGA/DTA Analyzer DTG-60AH, in the 25-900 $^{\circ}\text{C}$ temperature range, using a platinum crucible with *ca.* 8.0 mg of sample, under dynamic nitrogen atmosphere (30 mL min^{-1}) and with a heating rate of 10 K min^{-1} . FT-IR spectra were recorded from KBr pellets (in the 400-4000 cm^{-1} spectral range) using a BRUKER IFS 66.

Powder X-rays diffraction was collected at room temperature on a Bruker D8 Focus Diffractometer (Cu $\text{K}_{\alpha 1,2}$ X-radiation, $\lambda_1=1.540598 \text{ \AA}$ and $\lambda_2=1.544426 \text{ \AA}$), equipped with a flat-plate sample holder in a

Bragg-Bretano para-focus optics configuration (40 kV, 50 mA). Intensity was collected in continuous mode ($3 \leq 2\theta \leq 50^\circ$) by the step-continuous method (step= 0.01°). The Rietveld refinement^[1] for R and *G-Marker* were performed with the software GSAS/EXPGUI,^[2, 3] using as starting premise the atomic coordinates of the structural model previously reported.^[4] The preferential orientation was corrected using spherical harmonic model (sixth order) proposed by Jarvinen,^[5] the peak profile was adjusted by Thompson-Cox-Hastings function^[6] modified by Young and Desai (pV-TCHZ),^[7] surface roughness correction was refined by Pitschke function^[8] and background was fitted by an eighth-degree shifted Chebyshev polynomial function. In the final runs, the following parameters were refined: scale factor, background and absorption coefficients, spherical harmonic, unit-cell parameters and pV-TCHZ correction for asymmetric parameters.

MCF-7 (human breast adenocarcinoma cell) A549 (adenocarcinomic human alveolar basal epithelial cells), Caco-2 (human epithelial colorectal adenocarcinoma cells) and primary culture cells taken from healthy human dental pulp consisting mainly of fibroblasts (normal control) cells (3×10^3 /well) were seeded in 96 well plate and treated for 72 h with nine DHPM derivatives (see concentration in the main text). Shorter treatment times (24 h and 48 h) also were performed using MCF-7 cells as a model. Compounds that were effective for at least 2 cells lines were aggregated and tested on intermediate concentrations against its respective cancer cells lines, following 72 h of treatment. Also it was determined time dependency effect to all tested compound against MCF-7 cells and to compounds that showed the most effective reduction of A549 and Caco-2 cells viability. Monastrol (1 mM) was used as positive control in all assays. The cytotoxicity was determined using 3-(4,5-dimethylthiazol-2-yl)-2,5-diphenylterazolium bromide MTT according to the manufacturer's instructions. The absorbance readings were performed by spectrophotometer (SpectraMax M5, Molecular Devices - Sunnyvale, California, USA). Cell viability was normalized to control (vehicle alone). Statistical analyses were performed using GraphPad Prism 5 Software. Statistical significance of differences was determined by ANOVA with post-hoc comparison by Dunnett's test. A P value <0.05 was considered statistically significant.

General procedure for the Biginelli reaction.

(a) Batch conditions.

A sealed Schlenk tube containing 1.00 mmol of aldehyde, 1.00 mmol of 1,3-dicarbonyl compound, 1.00 of urea (or thiourea), and CP 1 (5 mol %, ≈15 mg) was allowed to react at 100 °C for 5 hours. Products were purified by chromatographic column eluted with mixtures of hexane/ethyl acetate

or, if the product precipitates in the reaction medium, it is filtered and washed with cold ethanol followed by consecutive crystallizations from the methanolic solution. See yields in Tables 2 and 4.

(b) Continuous flow conditions.

A stock solution tube containing 1.00 mmol of aldehyde, 1.00 mmol of 1,3-dicarbonyl compound, 1.00 of urea (or thiourea) and 5 mL of DMF was prepared and pumped through a packed bed reactor containing 250 mg of catalyst **1** (50 mm x 6.6 mm) at different temperatures and residence times. Samples were taken and analysed by CG-MS, followed by isolation and purification when necessary.

Ethyl-6-methyl-2-oxo-4-phenyl-1,2,3,4-tetrahydropyrimidine-5-carboxylate (**4a**): ^1H NMR (DMSO-*d*₆, 300 MHz, δ ppm): 9.22 (s, 1H), 7.76 (s, 1H), 7.29 - 7.18 (m, 5H), 5.14 (s, 1H), 3.97 (q, 2H, $J = 6.8$ Hz), 2.24 (s, 3H), 1.07 (t, 3H, $J = 6.8$ Hz). ^{13}C NMR (DMSO-*d*₆, 75 MHz, δ ppm): 165.7, 152.6, 148.8, 145.3, 128.8, 127.7, 126.7, 99.7, 59.6, 54.4, 18.2, 14.5. FT- IR (KBr, cm^{-1}): 3252, 3109, 2972, 1728, 1689, 1645, 1468, 1230, 1097, 778. White solid, m.p. 211-213 °C (literature¹ 212-213 °C) and R_f 0.60 (Hexane/AcOEt 7:3).

Ethyl-6-methyl-4-phenyl-2-thioxo-1,2,3,4-tetrahydropyrimidine-5-carboxylate (**4b**): ^1H NMR (DMSO-*d*₆, 300 MHz, δ ppm): 11.15 (s, 1H), 10.44 (s, 1H), 8.31- 8.04 (m, 5H), 5.94 (d, 1H, $J = 3.0$ Hz), 4.75 (q, 2H, $J = 6.7$ Hz), 3.05 (s, 3H), 1.84 (t, 3H, $J = 7.1$ Hz). ^{13}C NMR (DMSO-*d*₆, 75 MHz, δ ppm): 174.7, 166.9, 165.4, 145.9, 130.1, 129.0, 128.8, 100.7, 60.1, 53.9, 17.7, 14.6. FT-IR (KBr, cm^{-1}): 3322, 3466, 3176, 3111, 1670, 1575, 1470, 1277, 1197, 1105, 696. Yellow solid, m.p. 201-202 °C (literature¹ 200-202°C) and R_f 0.50 (Hexane/AcOEt 7:3).

Ethyl-4-(3-hydroxyphenyl)-6-methyl-2-oxo-1,2,3,4-tetrahydropyrimidine-5-carboxylate (**4c**): ^1H NMR (DMSO-*d*₆, 300 MHz, δ ppm): 10.14 (s, 1H), 9.93 (s, 1H), 8.46(s, 1H), 7.65 (t, 1H, $J = 7.9$ Hz), 7.44-7.36 (m, 3H), 5.82 (d, 1H, $J = 2.7$ Hz), 4.76 (q, 2H, $J = 7.2$ Hz), 2.99 (s, 3H), 1.87 (t, 3H, $J = 7.1$ Hz). ^{13}C NMR (DMSO-*d*₆, 75 MHz, δ ppm): 165.9, 157.8, 152.7, 148.6, 146.7, 129.8, 128.8, 117.3, 114.6, 99.8, 59.6, 54.3, 18.2, 14.6. FT-IR (KBr, cm^{-1}): 3514, 3364, 3250, 3104, 2978, 1722,

1638, 1600, 1475, 1305, 1221, 1056, 771. White solid, m.p. 169-170 °C (literature¹ 168-170 °C) and Rf 0.33 (Hexane/AcOEt 7:3).

Ethyl 6-methyl-4-(3-hydroxyphenyl)-2-thioxo-1,2,3,4-tetrahydropyrimidine-5-carboxylate (**4d**): ¹H NMR (DMSO-*d*₆, 300 MHz, δ ppm): 10.28 (s, 1H), 9.59 (s, 1H), 9.44 (s, 1H), 7.09 (t, 1H, *J* = 7.9 Hz), 6.65 (m, 3H), 5.09 (d, 1H, *J* = 2.7 Hz), 3.98 (q, 2H, *J* = 6.7 Hz), 2.27 (s, 3H), 1.08 (t, 3H, *J* = 6.9 Hz). ¹³C NMR (DMSO-*d*₆, 75 MHz, δ ppm): 174.6, 165.6, 157.9, 145.6, 145.2, 129.9, 117.5, 115.0, 113.8, 101.2, 60.5, 54.4, 17.6, 14.4. FT-IR (KBr, cm⁻¹): 3304, 3179, 3109, 2982, 1662, 1573, 1479, 1375, 1293, 1196, 1117, 747. Yellow solid, m.p. 181-182 °C (literature¹ 180-181 °C) and Rf 0.24 (Hexane/AcOEt 7:3).

Ethyl-6-methyl-4-(3-nitrophenyl)-2-oxo-1,2,3,4-tetrahydropyrimidine-5-carboxylate (**4e**): ¹H NMR (DMSO-*d*₆, 300 MHz, δ ppm): 9.39 (s, 1H), 8.16- 7.68 (m, 4H), 3.89 (q, 2H, *J* = 2.7 Hz), 2.28 (s, 3H), 1.10 (t, 3H, *J* = 6.9 Hz). ¹³C NMR (DMSO-*d*₆, 75 MHz, δ ppm): 165.1, 151.8, 149.5, 147.7, 147.0, 133.0, 130.3, 122.4, 121.0, 98.3, 59.4, 53.6, 17.9, 14.0. FT-IR (KBr, cm⁻¹): 3330, 3213, 3105, 2965, 1709, 1631, 1520, 1456, 1343, 1221, 1084, 810, 686, 530. White solid, m.p. 241-242 °C (literature¹ 240-242 °C) and Rf 0.85 (Hexane/AcOEt 7:3).

1,2,3,4-tetrahydro-6-methyl-2-oxo-5-pyrimidinecarboxylic acid ethyl ester (**4f**): ¹H NMR (DMSO-*d*₆, 300 MHz, δ ppm): 4.58 (q, 2H, *J* = 3.7 Hz), 3.43 (d, 2H), 1.07 (t, 3H, *J* = 7.0 Hz). FT-IR (KBr, cm⁻¹): 3356, 2928, 1621, 1571, 1242, 664. White solid, m.p. 257-258 °C (literature¹ 258-259 °C).

1,2,3,4-tetrahydro-4-(4-hydroxy-3-methoxyphenyl)-6-methyl-2-oxo-5-pyrimidinecarboxylic acid ethyl ester (**4g**): ¹H NMR (DMSO-*d*₆, 300 MHz, δ ppm): 9.15 (s, 1H), 8.91 (s, 1H), 7.67 (s, 1H), 6.81-6.65 (m, 3H), 5.09 (s, 1H), 4.44 (q, 2H), 3.99 (s, 3H), 2.46 (s, 3H), 1.06 (t, 3H, *J* = 5.2 Hz). ¹³C NMR (DMSO-*d*₆, 75 MHz, δ ppm): 165.9, 152.9, 148.2, 147.7, 146.19, 136.3, 118.0, 115.7, 111.2, 100.1, 59.6, 55.9, 54.0, 18.1, 14.5. FT-IR (KBr, cm⁻¹): 3542, 3242, 3115, 2972, 2922, 1703, 1642, 1509, 1219, 1086, 782. White solid, m.p. 229-231 °C (literature¹ 228-231 °C) and Rf 0.85 (Hexane/AcOEt 7:3).

2,3,4,6,7,8-hexahydro-4-(3-hydroxyphenyl)-2-thioxo-quinazolin-5(1H)-one (**4h**): ¹H NMR (DMSO-*d*₆, 300 MHz, δ ppm): 10.57 (s, 1H), 9.64 (s, 1H), 9.42 (s, 1H), 7.10-7.05 (m, 4H), 5.08 (d, *J* = 3.3 Hz), 3.38 (s, 1H), 2.47 (q, 1H, *J* = 4.2 Hz), 1.96 (s, 1H). ¹³C NMR (DMSO-*d*₆, 75 MHz, δ ppm): 194.4, 184.2, 174.8, 157.8, 151.0, 145.1, 129.9, 117.4, 113.7, 109.5, 52.1, 36.8, 25.7, 20.9. FT-IR (KBr, cm⁻¹): 3408, 3284, 2916, 1620, 1447, 1356, 1175, 760. Yellow solid, m.p. 228-229 °C (literature¹ 229-230 °C) and R_f 0.81 (MeOH).

2,3,4,6,7,8-hexahydro-4-(3-hydroxyphenyl)-7,7-dimethyl-2-thioxo-5(1H)-quinazolinone (**4i**): ¹H NMR (DMSO-*d*₆, 300 MHz, δ ppm): 10.56 (s, 1H, NH), 9.57, 9.23, 7.14- 6.63 (m, 4H), 5.07 (d, 1H, *J* = 3.3 Hz), 1.99 (s, 2H), 1.74, 1.19 (s, 3H). ¹³C NMR (DMSO-*d*₆, 75 MHz, δ ppm): 196.7, 194.3, 184.2, 174.8, 157.8, 151.0, 145.1, 129.9, 117.4, 109.5, 52.1, 36.8, 32.4, 25.7, 20.9. FT-IR (KBr, cm⁻¹): 3400, 2957, 1644, 1585, 1463, 1364, 1193, 793, 692, 472. Yellow solid, m.p. 219-221 °C (literature¹ 220 °C) and R_f 0.17 (Hexane/AcOEt 7:3).

4-(1,3-benzodioxol-5-yl)-1,2,3,4-tetrahydro-6-methyl-2-thioxo-5-pyrimidinecarboxylic acid- ethyl ester (**4j**): ¹H NMR (DMSO-*d*₆, 300 MHz, δ ppm): 10.34 (s, 1H), 9.63 (s, 1H), 6.88 (s, 1H), 6.72 (d, 2H, *J* = 1.5 Hz), 6.00 (s, 2H), 5.09 (d, 1H, *J* = 3.6 Hz), 2.29 (s, 3H), 1.12 (t, 3H). ¹³C NMR (DMSO-*d*₆, 75 MHz, δ ppm): 174.4, 166.5, 147.8, 147.1, 145.5, 137.8, 134.1, 120.1, 108.6, 107.2, 101.5, 60.0, 54.1, 17.6, 14.5. FT-IR (KBr, cm⁻¹): 3320, 3185, 2978, 2892, 1163, 1573, 1492, 1336, 1235, 1202, 1107, 742. Yellow solid, m.p. 173-175 °C (literature¹ 174-175 °C) and R_f 0.55 (Hexane/AcOEt 7:3).

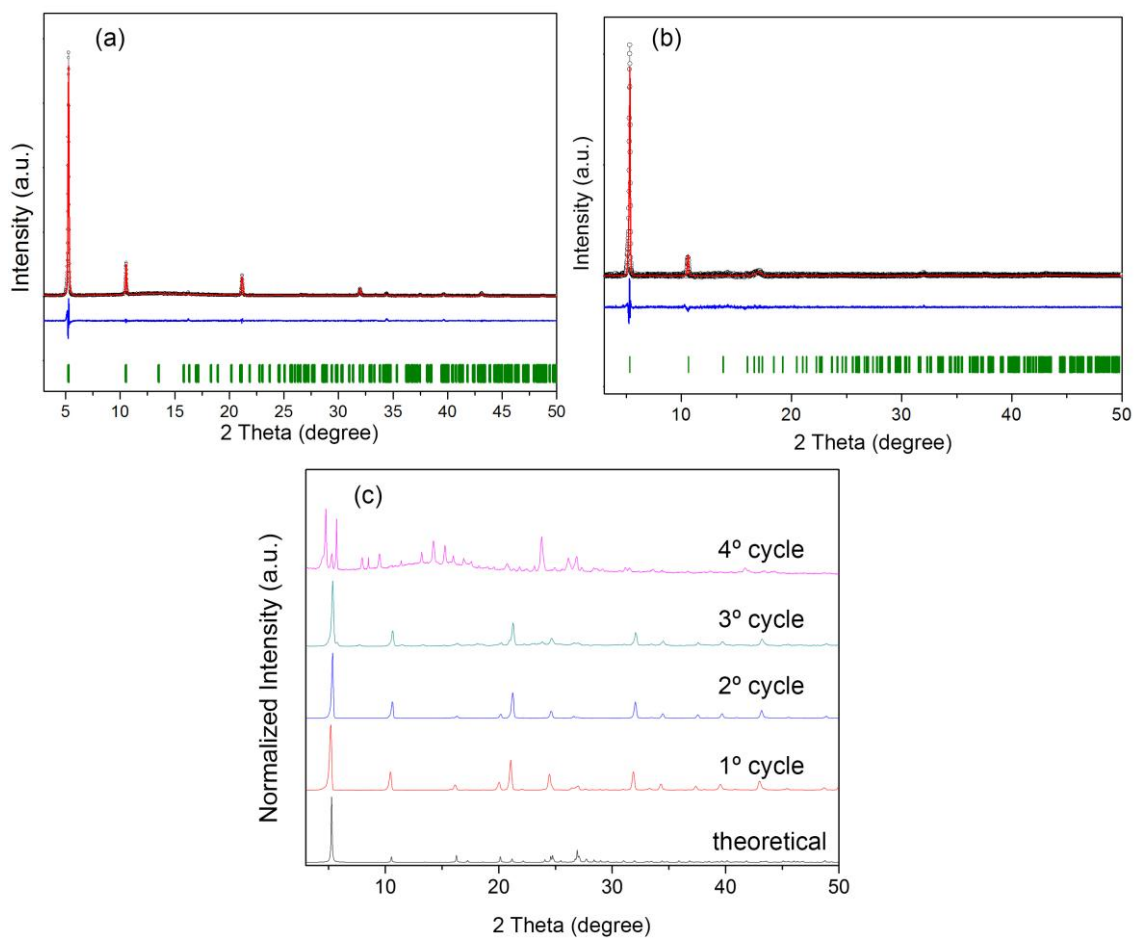


Figure S1. (a) and (b) Final Rietveld of **1** and **2**. Observed data points are indicated as black circles, the best-fit profile (upper trace) and the difference pattern (lower trace) are drawn as solid red and green lines, respectively. Blue vertical bars indicate the angular positions of the allowed Bragg reflections. Reliability Factors for refinement: R_p : 1.32/1.50; R_{wp} : 6.11/5.32 χ^2 : 7.56/ 8.23; R_F^2 : 8.43/9.23 for **1** and **2** respectively. (c) Solid black, red, cyan and magenta lines indicate the theoretical and experimental X-ray powder patterns acquired upon each catalytic cycle for **1**.

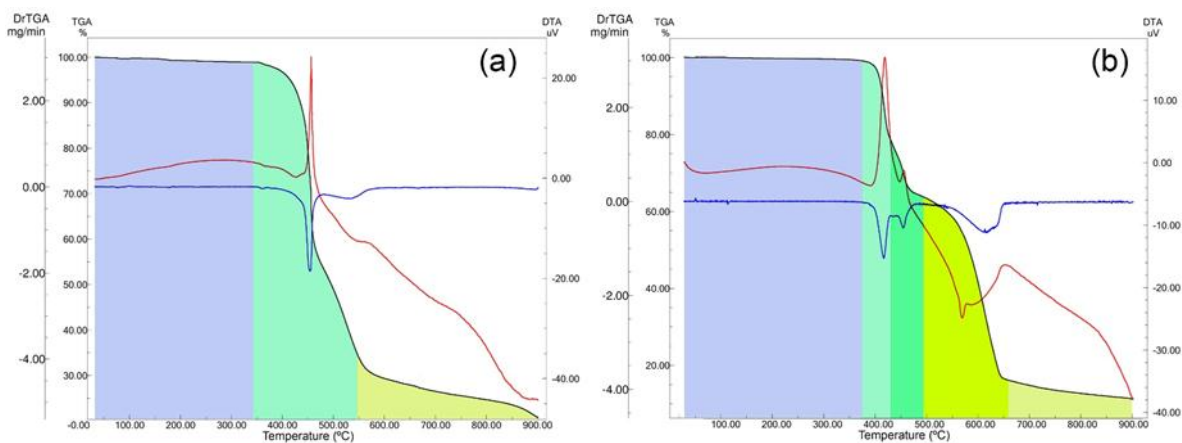


Figure S2. Thermogravimetric analysis for (a) **1** and (b) **2**. TGA, DTG and DTA curves are represented by solid black, blue and red lines, respectively.

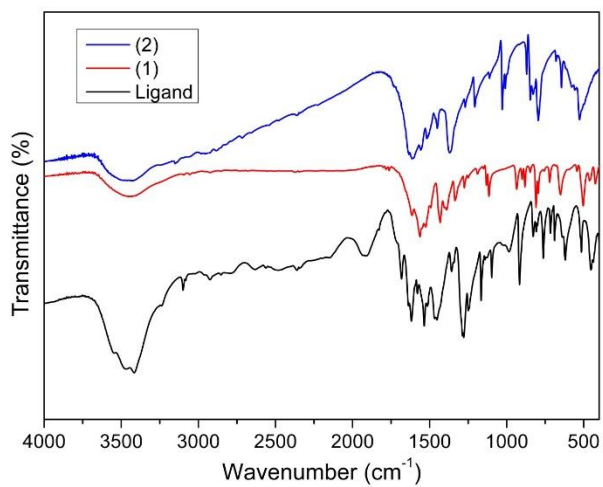


Figure S3. FT-IR spectrum. Ligand (black), **1** (red) and **2** (blue).

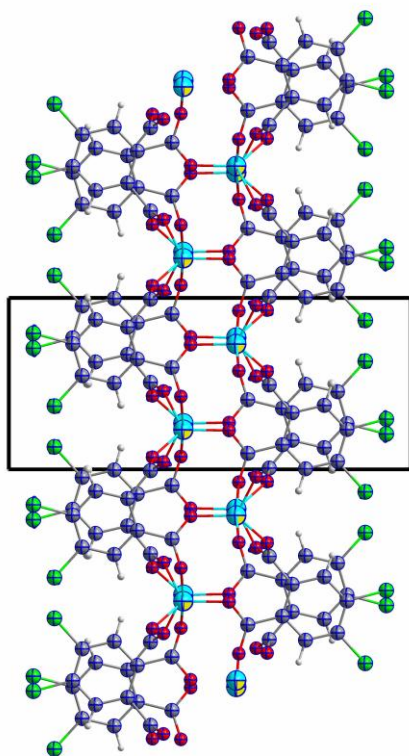


Figure S4. Crystal structure of **1**. Projection along of *b* axis.

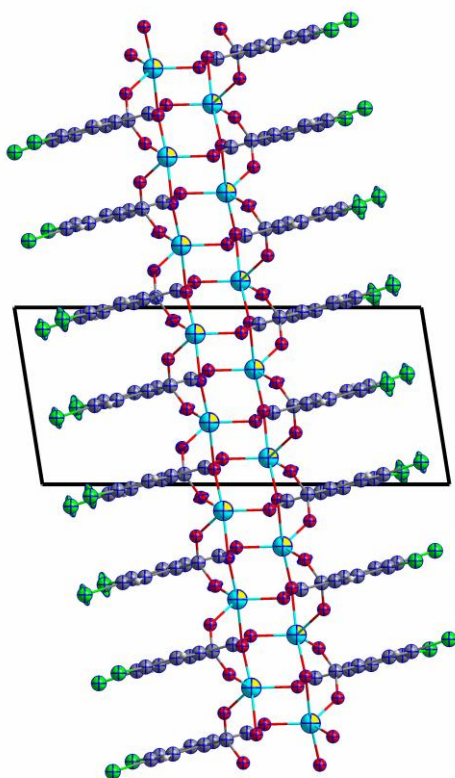


Figure S5. Crystal structure of **1**. Projection along of *c* axis.

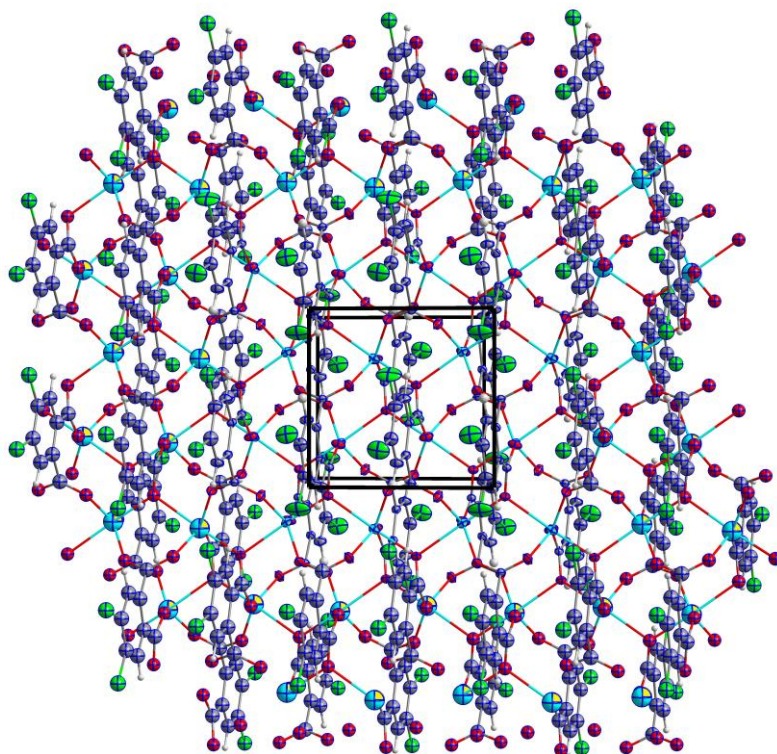


Figure S6. Crystal structure of **1**. Projection along of *a* axis.

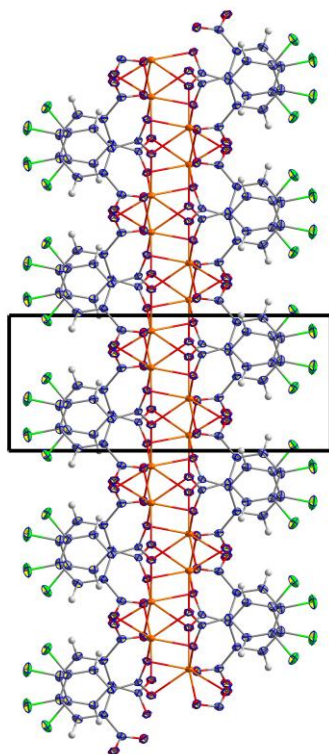


Figure S7. Crystal structure of **2**. Projection along of *b* axis.

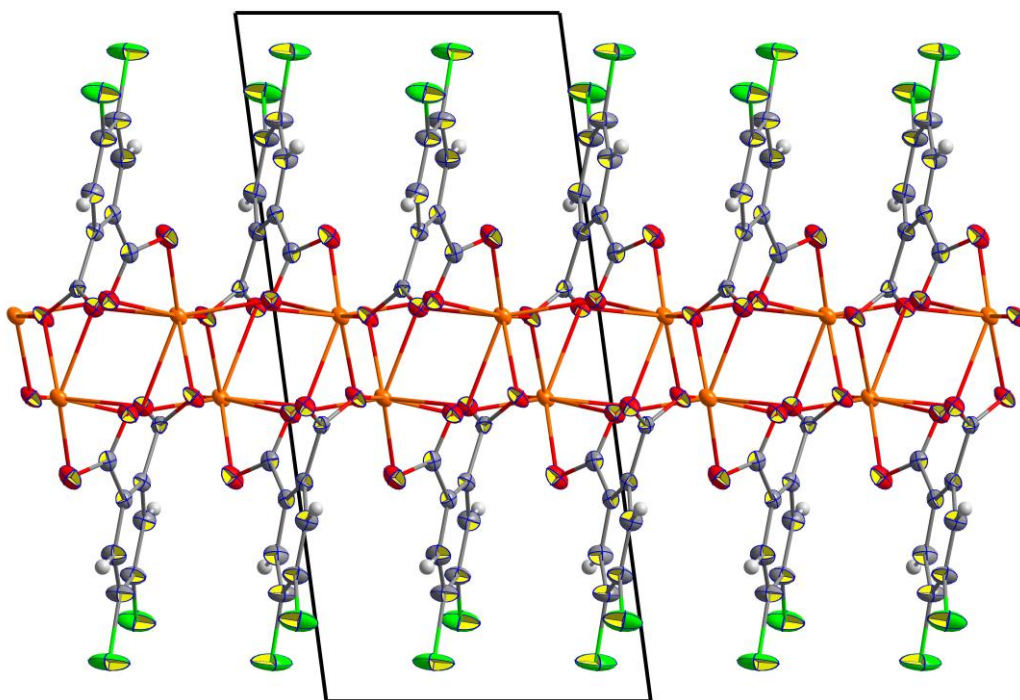


Figure S8. Crystal structure of **2**. Projection along of *c* axis.

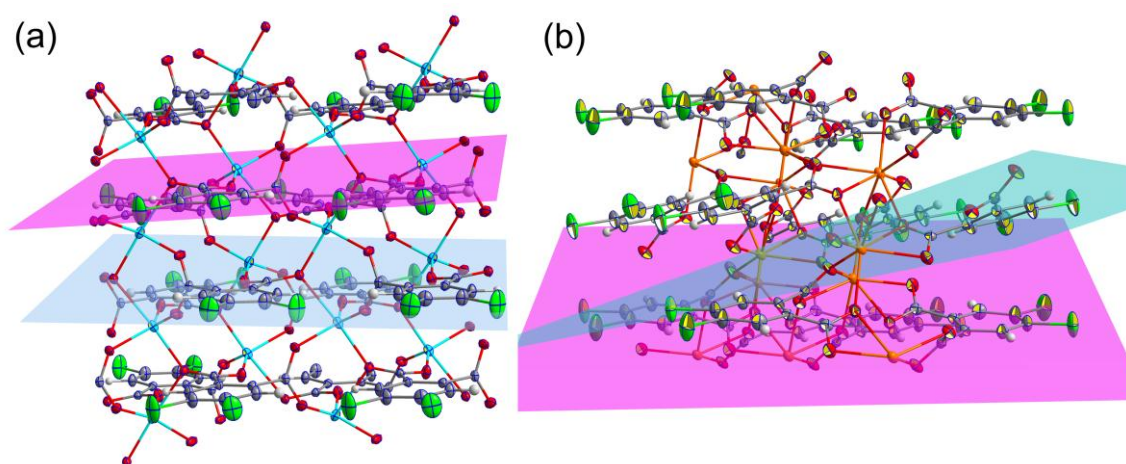


Figure S9. Dihedral planes among aromatic rings for **1** (a) and **2** (b).

1. H. G. O. Alvim, T. B. de Lima, H. C. B. de Oliveira, F. C. Gozzo, J. L. de Macedo, P. V. Abdelnur, W. A. Silva and B. A. D. Neto, *ACS Catal.*, 2013, **3**, 1420-1430.